Electronic Supplementary information (ESI)

# A case study of tuning crystal polymorphs of organic semiconductor towards simultaneously improved optimized light emission and field-effect property

Dan Liu,[‡a,b] Chenguang Li,[‡b,c] Shujie Niu,[a,b] Yang Li,[b] Mengxiao Hu,[a,b] Qingyuan Li,[b] Weigang Zhu,[b] Xiaotao Zhang,[c] Huanli Dong,[b]* and Wenping Hu[b,c]

[a]*Beijing Key laboratory for Optical Materials and photonic Devices, Department of Chemistry, Capital Normal University, Beijing 100048, China*

[b]*Beijing National Laboratory for Molecular Science, Key Laboratory of Organic Solids, Institute of Chemistry, Chinese Academy of Sciences, Beijing 100190, China *E-mail: dhl522@iccas.ac.cn*

[c]*Collaborative Innovation Center of Chemical Science and Engineering (Tianjin) & Department of Chemistry, School of Science, Tianjin University, Tianjin 300072, China*

‡*DL and CL contributed equally to this work*

## Experimental Section

### *Materials and Instrumentations*

All reagents and solvents were used as received from commercial resources unless otherwise specified.$^1$H NMR and $^{13}$C NMR spectras were recorded using a Bruker ADVANCE 400 NMR Spectrometer. $^1$HNMR spectras were referenced to $CDCl_3$ (7.26 ppm). UV-*Vis* absorption spectras were measured by a Jasco V-570 spectrometer. Photoluminescence (PL) spectras were recorded on a Jasco FP-6600 spectrofluorometer. Optical and SEM morphology images of DABD crystals were conducted on an Olympus BX53 optical microscope and S-4800, respectively. The fluorescence microscopy images were obtained from a Leica DM4 M fluorescence microscope. CV was performed with a CHI660C electrochemistry station in acetonitrile solution with sample concentration of $10^{-3}$ Musing $Bu_4NPF_6$ as electrolyte, and using Pt as working electrode, platinum wire as auxiliary electrode, and a porous glass wick Ag/AgCl as pseudo-reference electrode. Single crystal data were obtained using a Single crystal X-ray diffraction (Rigaku ST Saturn724$^+$). The structures were analyzed by XRD (Rigaku D/max 2500), TEM images and the corresponding SAED patterns (JEOL-2100). OFET characteristics were measured with a Keithley 4200 SCS at the ambient condition.

## Preparation of DABD crystals for X-ray diffraction

Single crystals suitable for X-ray diffraction analysis were prepared using slow evaporation a saturated solution of chloroform : ethyl alcohol (v:v, 2:1), and toluene : ethyl alcohol (v:v, 2:1) for $\alpha$-phaseand $\beta$-phase crystals of DABD, respectively.

## Detailed process for SAED diffraction point index attribution

The index of diffraction spots in SAED patterns here is determined combining the corresponding single crystal data of materials. The detailed procedure is as following. Firstly, determining the unit cell in the SAED patterns and measuring the distance and angle of unit cell in SAED pattern; secondly, comparing the unit cell values with that of its single crystal data to indexing the diffraction spots; finally, further calculating and verifying the index values for the second time. Based on the above three steps, we indexed the diffraction spots of $\alpha$-phase crystal and $\beta$-phase crystal.

## Preparation of DABD crystals for OFETs

Through drop-casting DABD of chloroform and toluene solution on the OTS-treated $SiO_2$/Si wafer, the wafers were putted in a weighing bottle and evaporated spontaneously overnight. Well-defined of rhombic-sheets $\alpha$-phase ingle crystals and ribbon-shape $\beta$-phase single crystals were obtained, respectively, and then they were fabricated to the devices directly.

## Theoretical calculation for DABD crystal energy

In the calculation process, the vdW-DF proposed by Dion *et al*[1] is used to calculate the total energy per cell, which is implemented by the SIESTA package.[2] A double-zeta plus polarization basis set is used to describe the valence electron, and the crystal structure is from the CIF file.

## Fabrication of DABD crystal based OFETs

Bottom-gate top-contact OFETs based on individual $\beta$-phase single crystals were fabricated on the OTS-treated $SiO_2$ (300 nm)/Si substrates with Au as source and drain electrodes. Drain and source electrodes (100 nm) were deposited on the $\beta$-phase single crystals by a “glue the gold film” technique. Current–voltage ($I$–$V$) characteristics of $\beta$-phase single crystals based on OFETs were recorded with a Keithley-4200 SCS and in the clean Micromanipulator 6150 station and shielded box at room temperature in air.

## *Synthesis of compound (2)，(3) and DABD (4)*

### Trimethyl anthracenylethynylsilane (2)

9-Bromoanthracene (**1**) (2 g, 7.76 mmol), $Pd(PPh_3)_2Cl_2$ (525 mg, 0.75 mmol) and CuI (168 mg, 0.88 mmol) were dried under HV in a two-neck flask. Piperidine (6 mL), TEA (60 mL) and TMS-acetylene (3 mL) were added slowly, and the mixture was bubbled with argon for 10 minutes. Afterwards the reaction mixture was stirred and heated at 110°C overnight (17 h). Saturated $NH_4Cl$ solution (50 mL) was added and the resulting mixture was extracted with Hex (3x 75 mL). The organic phase was dried over $MgSO_4$ and the solvent was evaporated. The residue was subjected to column chromatography on silica gel (Hex + 0.5% toluene) to obtain the silane **2** as a yellow solid (1.58 g, 5.74 mmol, 74%).

**$^1$H NMR ($CDCl_3$)**: $\delta$ = 0.42 (s, 9H), 7.49 (t, *J* = 7.88 Hz, 2H), 7.60 (t, *J* = 7.50 Hz, 2H), 7.99 (d, *J* = 8.46 Hz, 2H), 8.42 (s, 1H), 8.55 (d, *J* = 8.64 Hz, 2H).**$R_f$**: 0.4 (Hex + 0.5% toluene).

### 9-Ethynylanhracene (3)

The silane **2** (1.24 g, 4.50 mmol) and potassium carbonate (4.29 g, 23.34 mmol) were combined in THF:MeOH (1:1, 90 mL). The mixture was stirred for 16 h and filtered through Celite. The filtrate was concentrated to yield 9-ethynylanthracene (**3**) (897 mg, 4.44 mmol, 99%) as a yellow solid. Due to the instability of this compound over prolonged storage, it is used directly for the following reaction.

**$^1$H NMR ($CDCl_3$)**: $\delta$ = 3.99 (s, 1H), 7.51 (t, *J* = 7.66 Hz, 2H), 7.59 (t, *J* = 7.48 Hz, 2H), 8.02 (d, *J* = 8.62 Hz, 2H), 8.47 (s, 1H), 8.58 (d, *J* = 8.84 Hz, 2H). **$R_f$**: 0.4 (Hex + 0.5% toluene).

### 9,9'-Dianthryldiacetylene (DABD) (4)

A mixture of **3** (0.44 g, 2.2 mmol), cupric acetate monohydrate (10.0 g), pyridine (20 mL) and MeOH (2 mL) was stirred for 3 h at 50 $^oC$. The insoluble material was collected by the filtration, and its washed with a small amount of methanol, water, and a small amount of ethanol, successively. The orange tiny cubes (0.40 g, 91%) was purified by flash chromatography (silica gel, mixtures of PE/DCM = 10:1) to afford the pure product **4**.

**$^1$H NMR ($CDCl_3$)**: $\delta$ = 7.49 (t, *J* = 7.36 Hz, 4H), 7.61 (t, *J* = 7.40 Hz, 4H), 8.00 (d, *J* = 8.38 Hz, 4H), 8.44 (s, 2H), 8.64 (s,*J* = 8.68 Hz, 4H). **$R_f$**: 0.2 (Hex +0.5% toluene).Anal. calcd for $C_{32}H_{18}$(%): C:95.49, H: 4.51. Found: C: 95.09%, H: 4.62%.

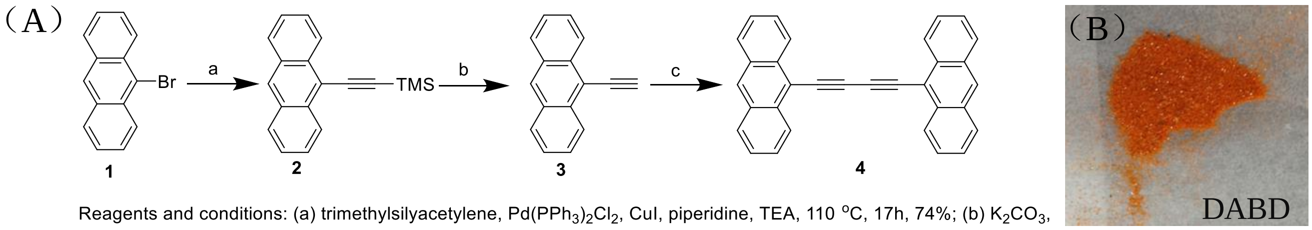

Reagents and conditions: (a) trimethylsilyacetylene, $Pd(PPh_3)_2Cl_2$, CuI, piperidine, TEA, 110 °C, 17h, 74%; (b) $K_2CO_3$, THF, MeOH, rt, 6h, 99%; (c) $Cu(OAc)_2 \cdot H_2O$, pyridine, MeOH, 50 °C, 3 h, 91%.

**Figure S1** Synthetic route to DABD (A) and powder of DABD (B).

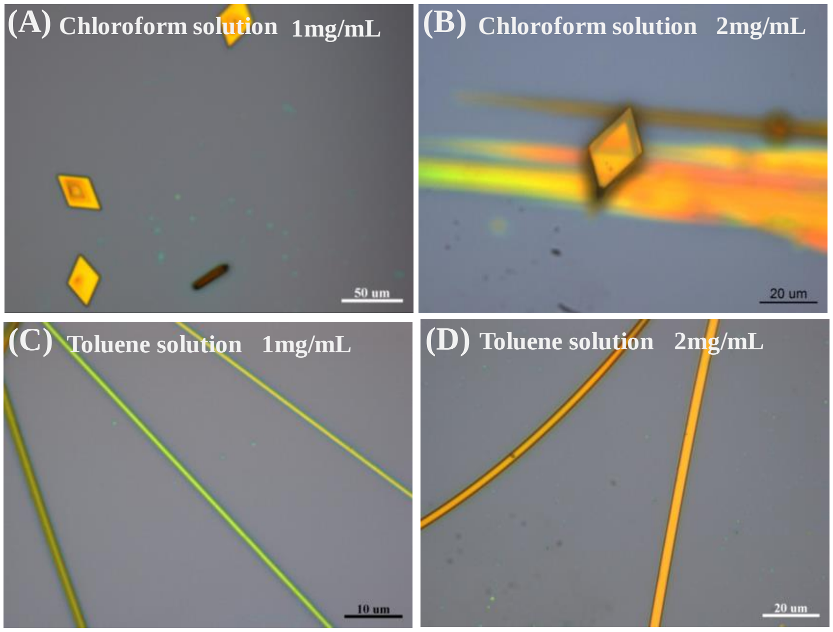

**Figure S2** Optical images of *α*-phase (A, B) and *β*-phase (C, D) of DABD crystals obtained from different solution concentrations.

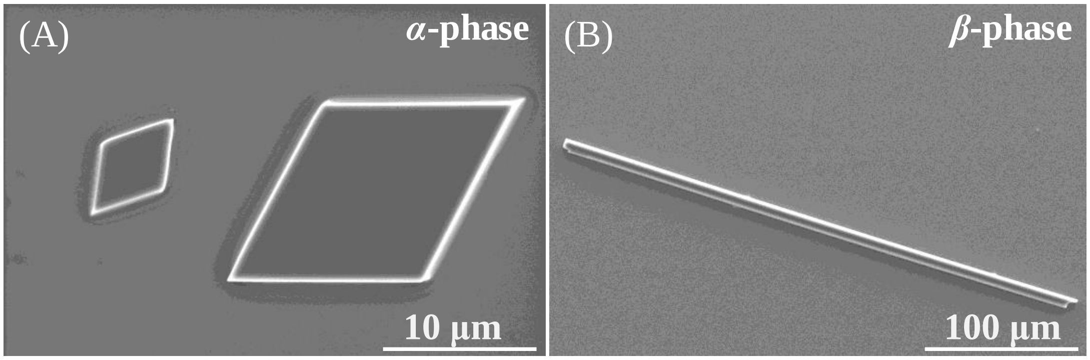

**Figure S3** SEM images of *α*-phase (A) and *β*-phase (B) of DABD crystals, respectively.

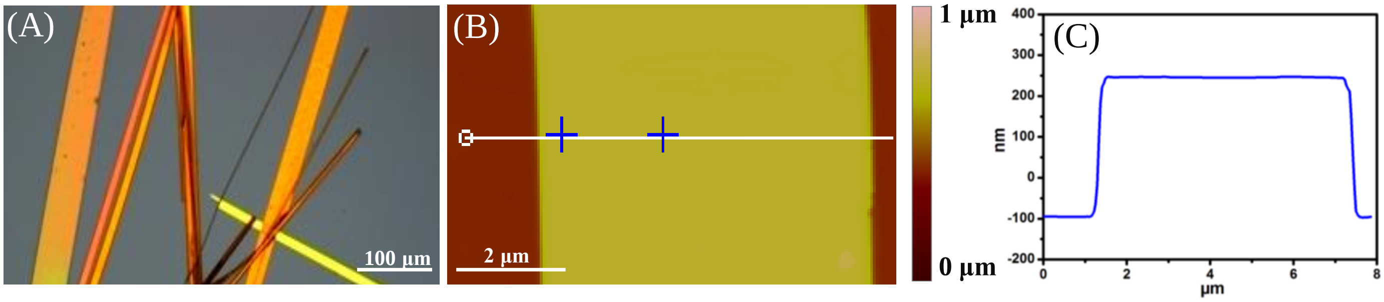

**Figure S4** (A) Optical microscopy image of *β*-phase crystalline nano-wires on the OTS-modified substrate. AFM morphology (B) and height (C) of individual the *β*-phase crystal.

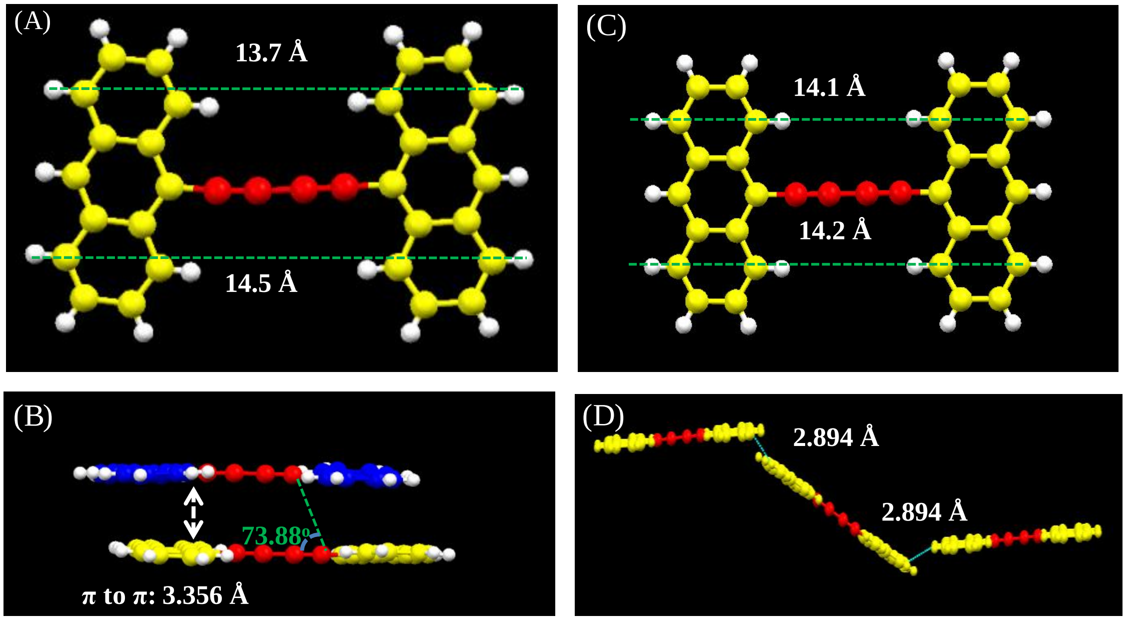

**Figure S5** The molecular structure (A) and the dimer structure (B) of *α*-phase crystals. The molecule structure (C) and short contact (D) of *β*-phase crystals.

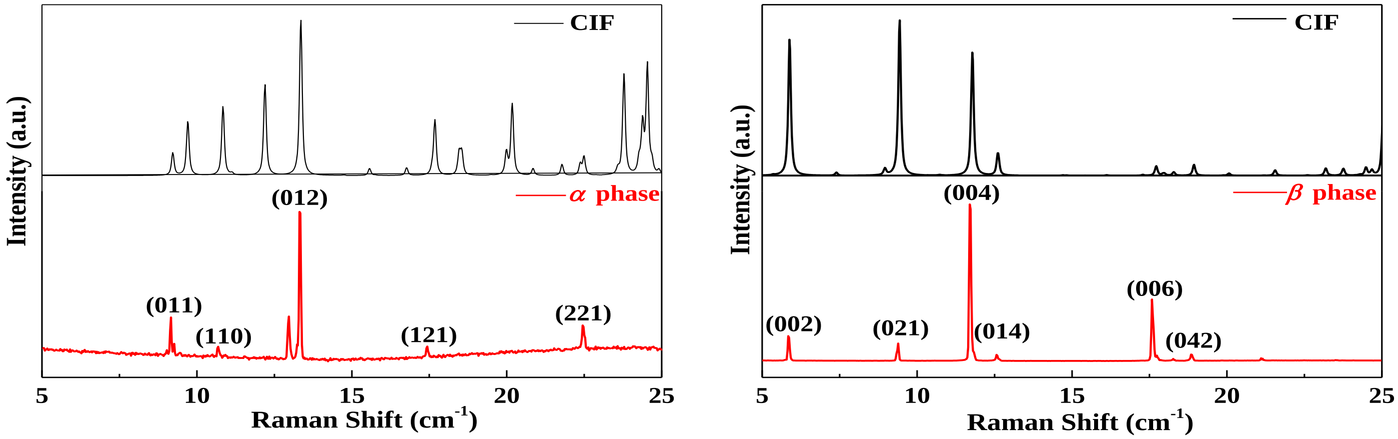

**Figure S6** XRD patterns of the *α*-phase (A) and *β*-phase (B) of DABD crystals.

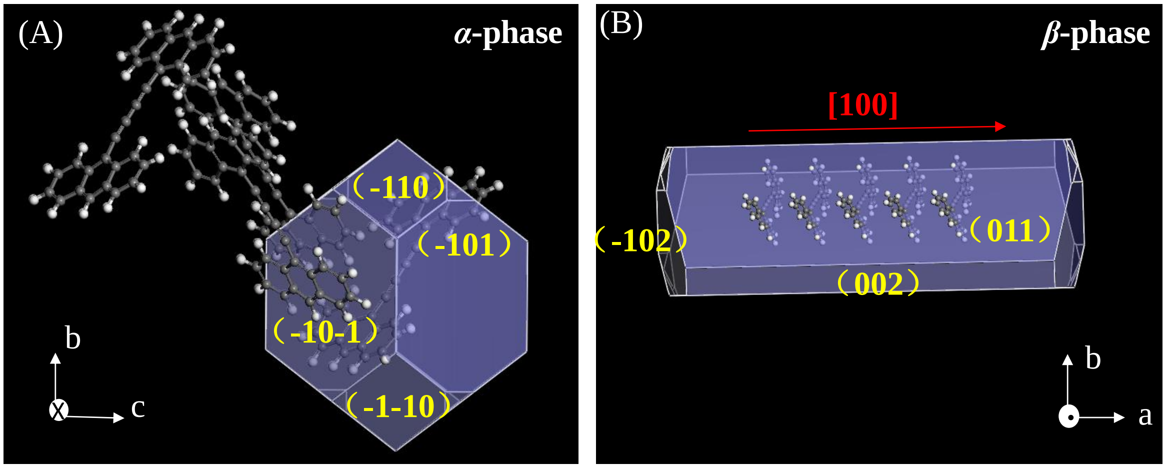

**Figure S7** The predicted equilibrium morphology of the *α*-phase DABD crystal (A) and *β*-phase DABD crystal (B).

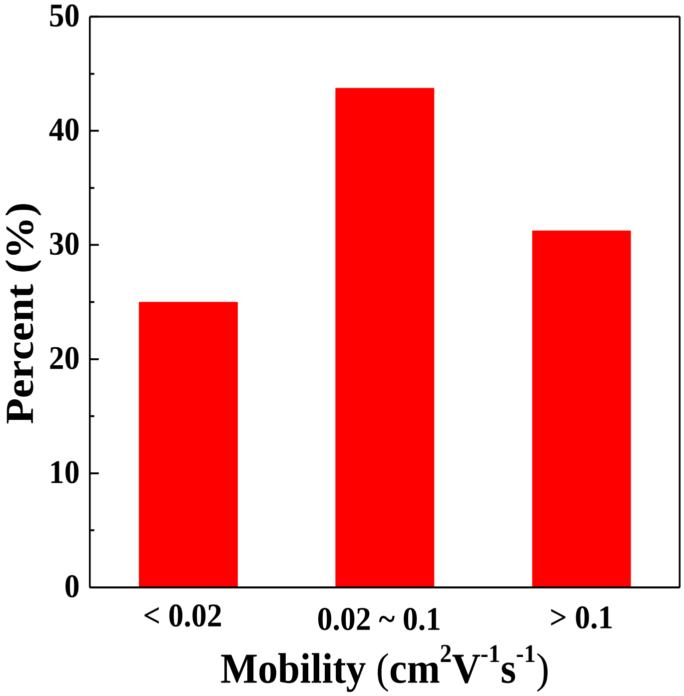

**Figure S8** Mobility distribution of 16 *β*-phase crystal-based transistors.

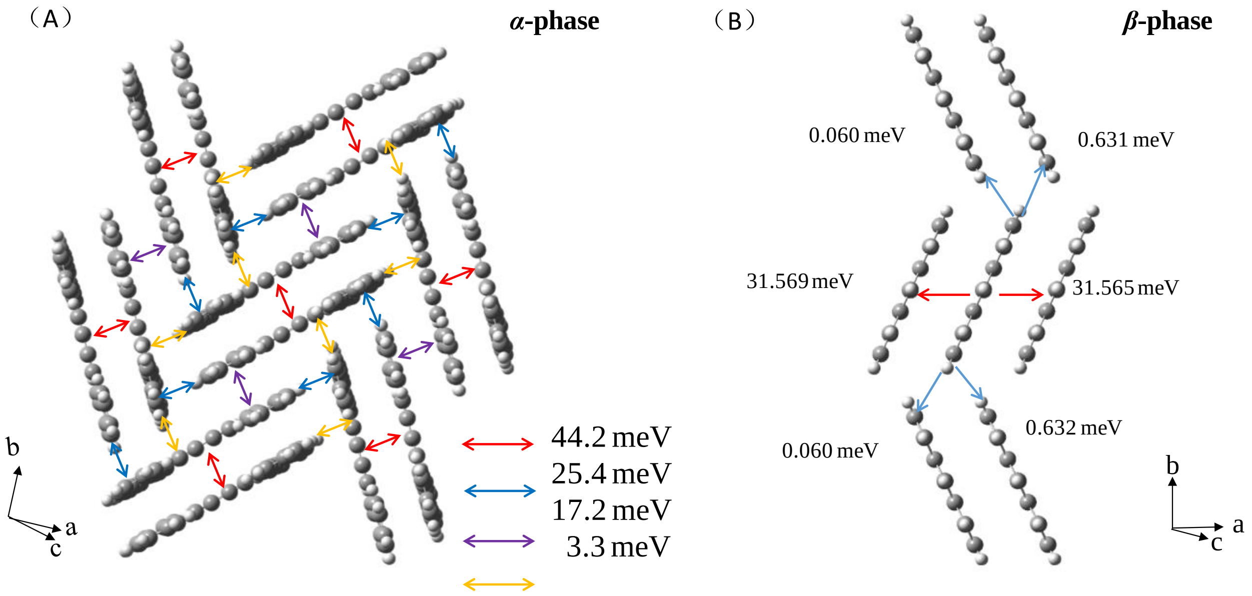

**Figure S9** Illustrations of transfer integrals calculated for the nearest neighboring molecular considered in the calculations for the *α*-phase (A) and *β*-phase (B) crystals of DABD, respectively. As for the *β*-phase crystals, although the transfer integrals in the edge-to-face direction is relatively small, the large transfer integral in the direction of [100], that is the conducting channel in the devices greatly contribute to the efficient charge transport.

**Table S1** Crystal data for the two phase of DABD

| Parameters | $\alpha$-phase (1034428) | $\beta$-phase (1864075) |
|---|---|---|
| Empirical formula | $C_{32}$ $H_{18}$ | $C_{32}$ $H_{18}$ |
| Formula weight | 402.46 | 402.46 |
| Temperature | 173.15 K | 173.15 K |
| Wavelength | 0.71073 Å | 0.71073 Å |
| Crystal system | Monoclinic | Orthorhombic |
| Space group | P 1 21/n 1 | P 21 21 21 |
| Unit cell dimensions | a = 11.097(2) Å, $\alpha$ = 90° | a = 3.94060(10) Å, $a$ = 90° |
| | b = 11.981(2) Å, $\beta$ = 90.23(3)° | b = 19.7156(5) Å, $\beta$ = 90° |
| | c = 15.854(3) Å, $\gamma$ = 90° | c = 30.0106(11) Å, $\gamma$ = 90° |
| Z | 4 | 4 |
| Density (calculated) | 1.268 g/cm$^3$ | 1.147 Mg/m$^3$ |
| Absorption coefficient | 0.072 mm$^{-1}$ | 0.065 mm$^{-1}$ |
| F(000) | 840 | 840 |
| Crystal size(mm) | 0.35 × 0.25 × 0.23 mm$^3$ | 0.467 × 0.141 × 0.109 mm$^3$ |
| Theta range for data collection | 3.401° to 27.482° | 1.705° to 27.495° |
| Index ranges | -14<=h<=14 | -4<=h<=5 |
| | -15<=k<=15 | -25<=k<=25 |
| | -20<=l<=20 | -38<=l<=38 |
| Reflections collected | 14161 | 16538 |
| Independent reflections | 4778 | 5057 |
| $R_{int}$ | 0.0405 | 0.0313 |
| Completeness to theta | 98.90% | 99.30% |
| Absorption correction | Semi-empirical from equivalents | None |
| Max. and min. transmission | 1.0000 and 0.8129 | None |
| Data/ restraints / parameters | 4778 / 0 / 289 | 5057 / 0 / 289 |
| Goodness-of-fit on $F^2$ | 1.209 | 1.082 |
| Final R indices [I>2sigma(I)] | $R_1$ = 0.0750 | $R_1$ = 0.0412, |
| | $wR_2$ = 0.1395 | $wR_2$ = 0.0964 |
| R indices (all data) | $R_1$ = 0.0854, | $R_1$ = 0.0553 |
| | $wR_2$ = 0.1453 | $wR_2$ = 0.1027 |
| Largest diff. peak and hole | 0.221 and -0.191 e. Å$^{-3}$ | 0.160 and -0.183 e. Å$^{-3}$ |

$^{1}$H NMR of **4** in CDCl$_3$

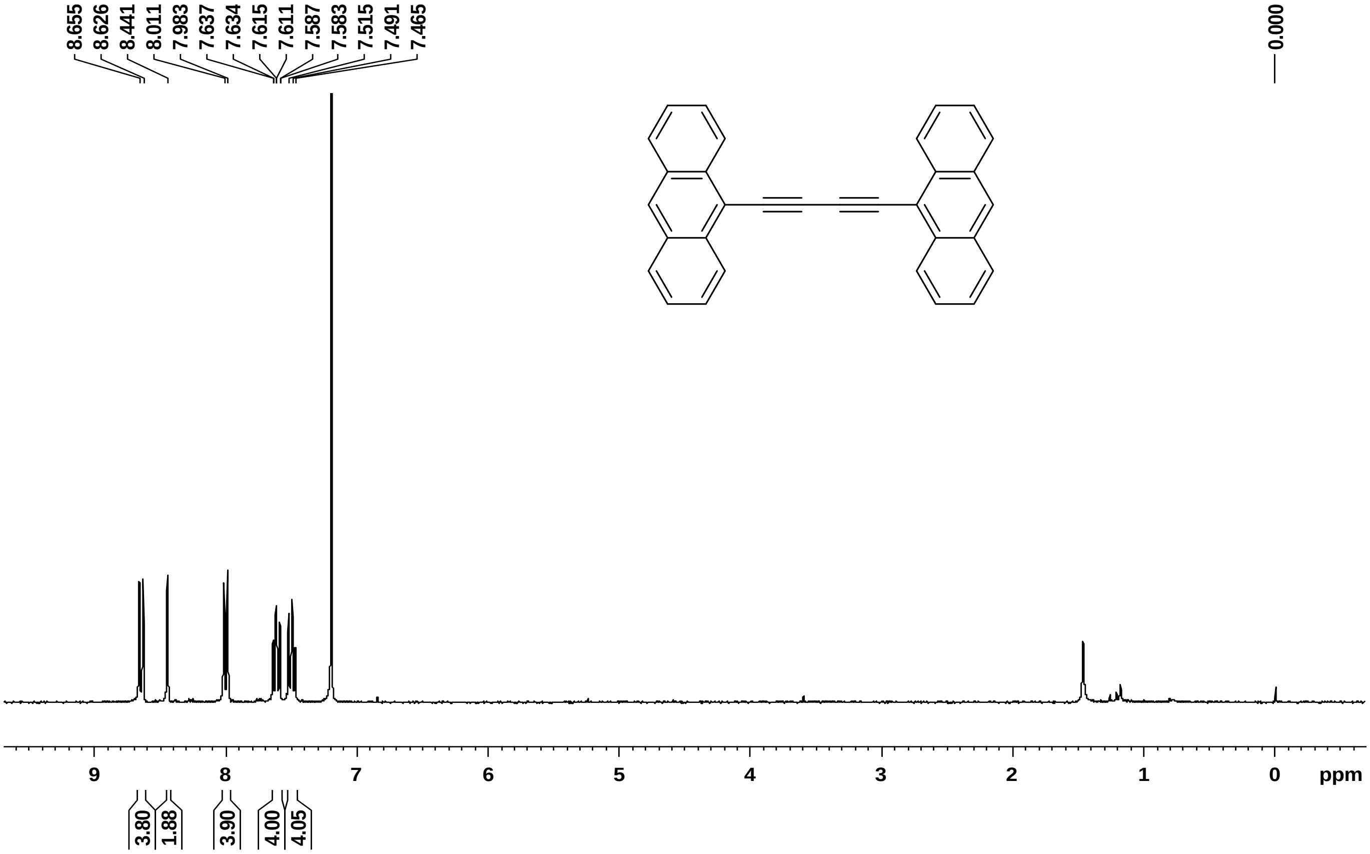

$^{1}$C NMR of **4** in CDCl$_3$

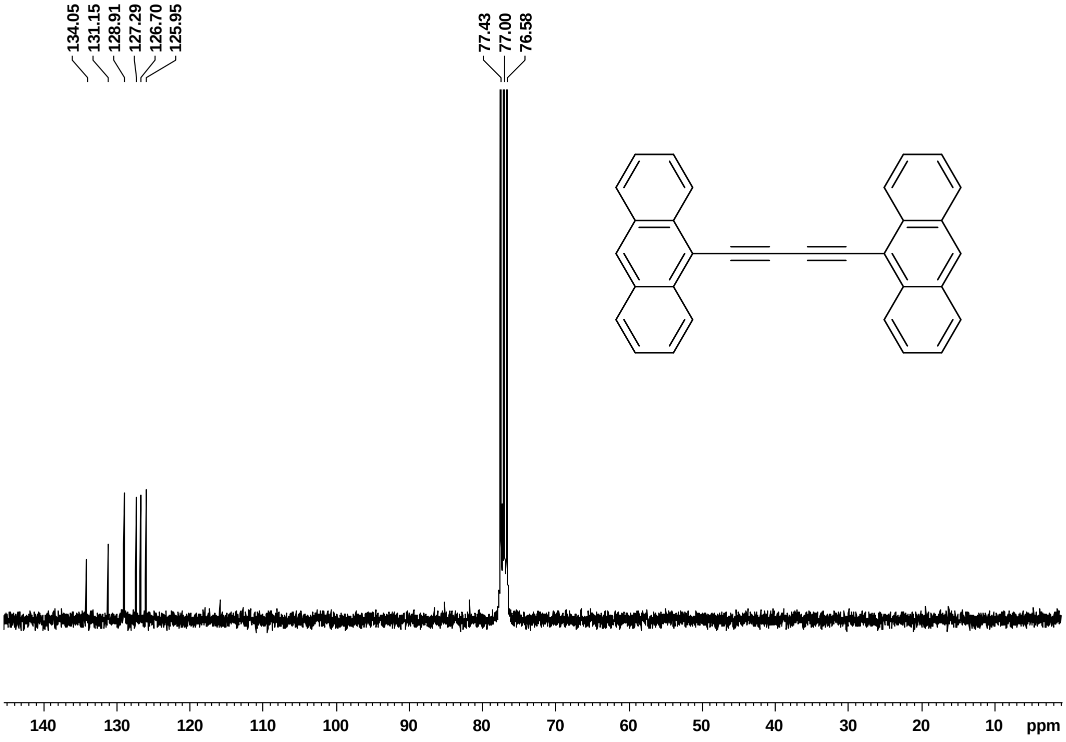

$^1$H NMR of **3** in CDCl$_3$

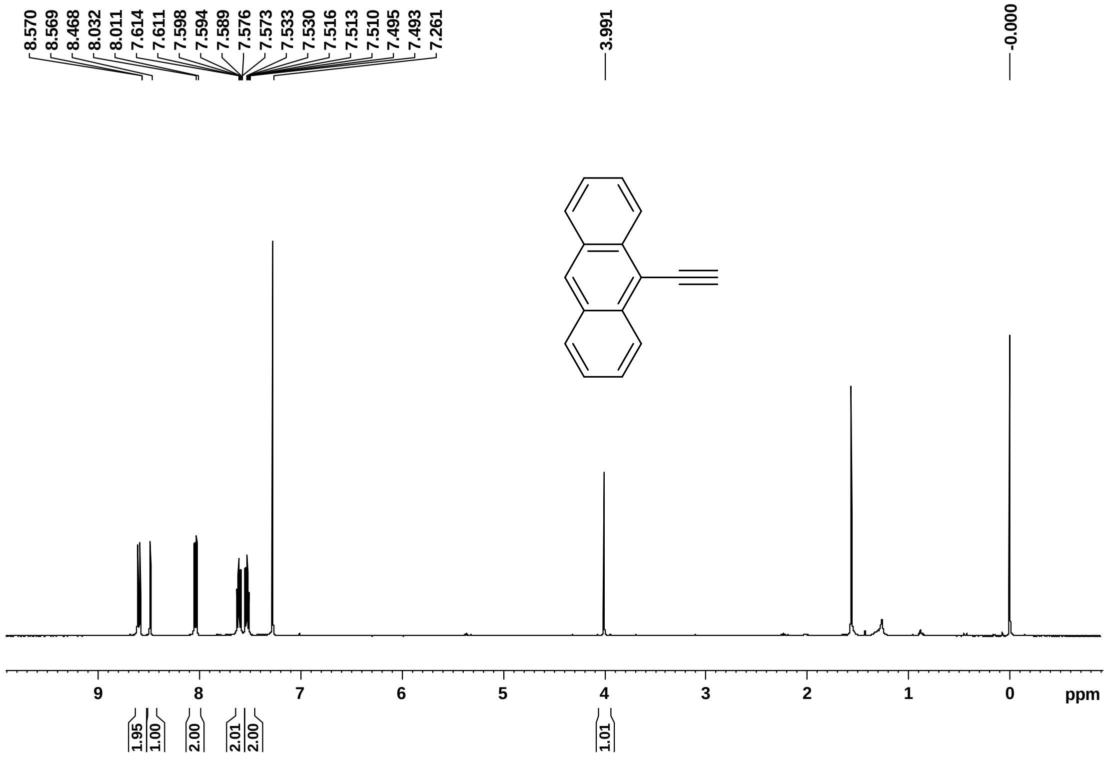

$^1$H NMR of **2** in CDCl$_3$

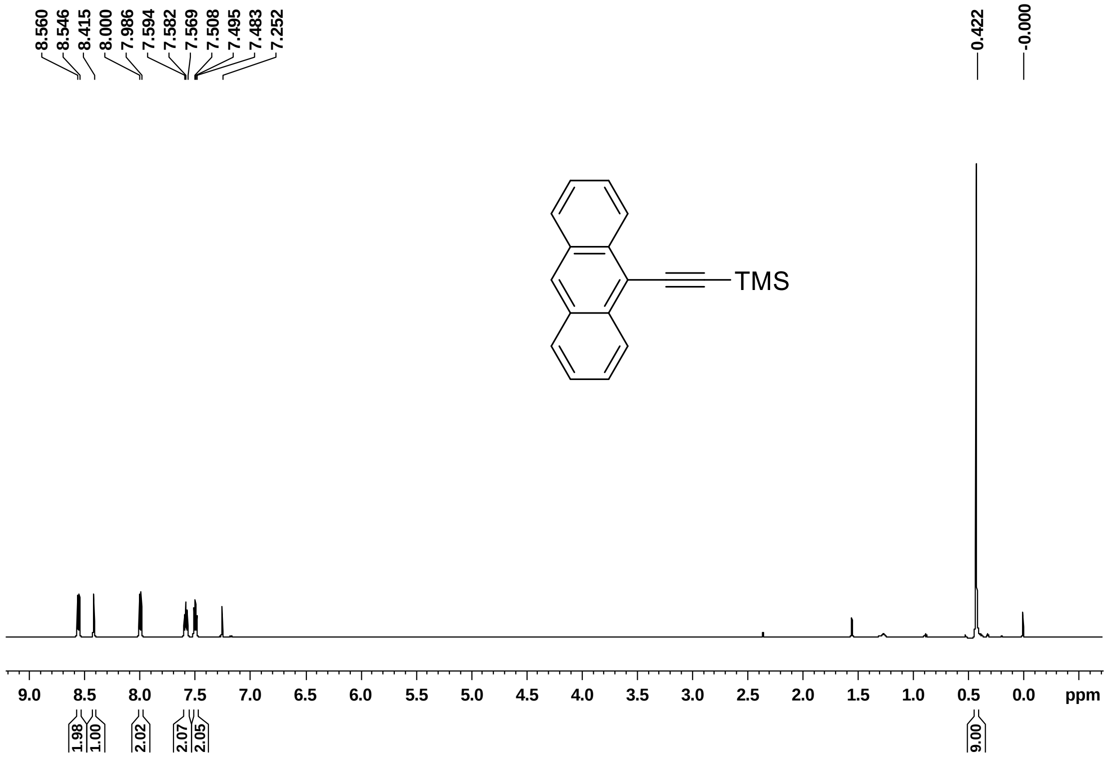

**References：**

1. M. Dion, H. Rydberg, E. Schro der, D. C. Langreth and B. I. Lundqvist, *Phys. Rev. Lett.*, 2004, *92*, 246401.
2. J. M. Soler, E. Artacho, J. D. Gale, A. Garcia, J. Junquera, P. Ordejon and D. S. Portal, *J. Phys. Condens. Matter.*, 2002, *14*, 2745.